Available online at www.sciencedirect.com

SCIENCE DIRECT®

Journal of the European Ceramic Society 26 (2006) 2899–2907

www.elsevier.com/locate/jeurceramsoc

Grain boundary reoxidation of donor-doped barium titanate ceramics

Hans Theo Langhammer[a,*], Darko Makovec[c], Yongping Pu[a,1], Hans-Peter Abicht[b], Miha Drofenik[c]

[a] Martin-Luther-Universität Halle-Wittenberg, FB Physik, D-06099 Halle (Saale), Germany
[b] Martin-Luther-Universität Halle-Wittenberg, FB Chemie, D-06099 Halle (Saale), Germany
[c] Jožef Stefan Institute, Department of Advanced Materials, SI-1111 Ljubljana, Slovenia

Abstract

The reoxidation process of donor-doped $BaTiO_3$ ceramics which is crucial for the development of the potential barrier at the grain boundary was investigated in situ by oxygen coulometry. Samples with nominal composition of $0.98Ba_{1-x}La_xTiO_3 + 0.02TiO_2$ ($0.0025 \leq x \leq 0.05$) were prepared by sintering under highly-reducing conditions and subsequently reoxidized by heating up to maximum 1380 °C at an oxygen partial pressure of 260 Pa. During the heating cycle three oxygen uptake peaks were observed. These effects could be attributed (1) to the filling up of oxygen vacancies which were formed during sintering, (2) to the transformation from the reduced to the oxidized phase of $BaTiO_3$ in the direct vicinity of the grain boundaries, and (3) to the formation of oxidized phase inside the grains which is controlled by oxygen bulk diffusion. Process (3) is accompanied with Ti-rich precipitations which were detected by TEM methods. The microscopic model of the development of the reoxidation process was confirmed by temperature-dependent dc and ac electrical measurements.

Keywords: $BaTiO_3$ and titanates; Grain boundaries; Oxygen coulometry; Electron microscopy; PTC devices

1. Introduction

In the wide field of applications of ferroelectric materials, e.g. capacitors, piezoelectric actuators and sensors, optical modulators, gas sensors and many others, those of them which are based mainly on grain boundary effects in polycrystalline or ceramic materials play an important role. Their working principle is often due to electronic transport processes which are controlled by the potential barriers at the grain boundaries. Examples are varistors, grain boundary barrier layer (GBBL) capacitors and resistors displaying a pronounced positive temperature coefficient of resistivity (PTCR) effect near the ferroelectric phase transition temperature. Commercially available PTCR materials base on $BaTiO_3$ and its solid solutions with other perovskites. Applications of the PTCR effect include self-controlling heaters, current limiters, TV degaussers and oxygen and temperature sensors. The PTCR effect is known more than 50 years and the first model which satisfactorily explains the general effect was developed in the early 1960s by Heywang.[1] Until now, a large number of papers on this subject have been published. An overview was given by Huybrechts et al.[2] Nevertheless, the physico-chemical processes which form the potential barrier at the grain boundary are still not understood in detail, and the tailoring and optimizing of the material properties is often an empirical task. One reason for this situation is the doping anomaly of donor-doped, air-sintered $BaTiO_3$ ceramics which means that the doping level is limited to a critical concentration of about 0.3 mol% if semiconductive material is desired. For donor concentrations above this critical value, which is rather independent on the kind of donor, the material becomes insulating and anomalous grain growth does not occur. In the past, several explanations for this anomaly were given.[3–6] Whereas the sudden decrease of the electrical conductivity often is attributed to the change of the donor compensation from an electronic to a vacancy mechanism, a satisfactory explanation of the abrupt change of microstructure was given by Drofenik.[7]

Due to the small donor concentrations of semiconductive $BaTiO_3$ (<0.5 mol%), direct observation of the influence of the doping elements by local microscopic investigations is difficult and the investigations were mainly restricted to macroscopic electrical properties and the overall microstructure like mean grain size. The increase of the critical donor concentration would overcome this limitation. It is well known that the critical con-

---

[*] Corresponding author. Tel.: +49 345 5525542; fax: +49 345 5527595.
E-mail address: langhammer@physik.uni-halle.de (H.T. Langhammer).

[1] Permanent address: Xi'an Jiaotong University, Xi'an, PR China.

doi:10.1016/j.jeurceramsoc.2006.02.006

centration depends on the oxygen partial pressure of the sintering atmosphere.[8,9] For example, by sintering in a reducing atmosphere of nitrogen containing 1% of hydrogen its value can be increased up to almost 10 mol%.[10] But the potential barrier at the grain boundaries of the reduced material shrinks due to the substantial increase in density of electronic charge carriers, since the oxygen vacancies formed are effective donors. Hence, the GBBL must be restored by a subsequent reoxidation process, which is significant for the development of the potential barrier and which normally takes place during the cooling cycle of the common sintering in air. Despite the increase of critical donor concentration, this procedure allows separate investigations of reoxidation and also grain growth. Formerly proposed by Hanke et al.,[11] it was systematically investigated by Makovec et al.[10] with respect to microstructural and electrical properties of $BaTiO_3$ ceramics doped with up to 10 mol% La. They proposed a structural model for GBBL ceramics describing the microstructure which consists of (1) a semiconducting bulk of the reduced phase of $BaTiO_3$ surrounded by (2) an outer shell of oxidized phase and (3) the actual grain boundary layer. This layer is characterized by adsorbed oxygen and/or intrinsic/extrinsic acceptor defects forming the negative space charge near the grain boundary which is necessary for the development of the potential barrier. The terms *reduced* and *oxidized phase*, respectively, correspond to donor-doped barium titanate where the donor is compensated either by electrons ($Ba_{1-x}D_x{}^{\bullet}Ti^{x/4+}{}_{1-x}Ti^{\prime/3+}{}_xO_3$) or by cation vacancies. Meanwhile, titanium vacancies are accepted as the predominant cation vacancies in donor-doped $BaTiO_3$ ($Ba_{1-x}D_x{}^{\bullet}Ti^{x/4+}{}_{1-x/4}(V_{Ti}{}^{\prime\prime\prime\prime})_{x/4}O_3$).[12,13] Another model with regions of higher (inner grain) and lower (outer grain region) oxygen vacancy concentration and a grain boundary region of oxidized phase was proposed by Morrison et al.[14] for 3.0 mol% La doped, air-quenched $BaTiO_3$.

To improve existing models and to get detailed knowledge about the thermodynamics and the kinetics of the several steps of the reoxidation process, in situ measurements of the oxygen exchange between specimen and ambient atmosphere should be helpful.

Thus, the aim of this paper is to show how such data can be gained by the method of oxygen coulometry applied during the reoxidation process. These measurements together with TEM investigations and temperature dependent impedance spectroscopy were used to derive a more detailed picture of the development of the inhomogeneous microstructure of donor-doped barium titanate ceramics and consequently of the development of the potential barrier at the grain boundaries.

2. Experimental

$BaTiO_3$ ceramics doped with La_{Ba} in a range of 0.25–5.0 mol% were prepared by conventional mixed-oxide technology. $BaTiO_3$ (Code 219-9, Lot 950097, Transelco, Pen Yan, NY, USA) was mixed with 2 mol% TiO_2 (Code 203-2, Transelco) and an adequate amount of La in an agate ball-mill according to the composition $0.98Ba_{1-x}La_xTiO_3 + 0.02TiO_2$. For the preparation of the 0.25 mol% La-doped $BaTiO_3$ samples, La was added as an aqueous solution of lanthanum acetate (P.A. grade, Fluka AG, Buchs, Switzerland), whereas for higher La concentrations, La was added as La_2O_3 (99.9%, Johnson Matthey, Cheshire, UK). The mixtures were granulated and uniaxially pressed into tablets (8 mm in diameter and ≈2 mm thick). The samples were sintered in a flow of 99% N_2–1% H_2 for 6 h at 1380 °C. For more details of the preparation see Ref. 10.

The sintered samples were subsequently reoxidized at an oxygen partial pressure of 260 Pa with different heating schedules (maximum temperature 1385 °C) at 10 K/min for heating and cooling. During reoxidizing the oxygen exchange between sample and surrounding was quantitatively monitored by a coulometric method based on oxygen conducting ZrO_2 Nernst cells (Zirox Sensoren & Elektronik GmbH, Greifswald, Germany, model SGM5-EL). The measuring principle is described elsewhere.[15] For each reoxidation run a total sample mass of about 1 g was used.

The microstructure of the samples before and after reoxidation were investigated by means of optical microscopy and TEM using a field-emission electron-source scanning-transmission electron microscope STEM (Model JEM 2010 F, JEOL, Tokyo, Japan), operated at 200 kV. Specimens for optical microscopy were prepared conventionally by polishing and chemical etching. Specimens for TEM were prepared by cutting 3 mm diameter discs from the ceramic samples. The discs were reduced to ∼120 μm by grinding. At the centre of the disc, a region about 20 μm thick was produced by a dimple grinder. Finally, specimens were thinned by argon-ion erosion at 4 kV with an incident angle of about 10°.

The electrical resistivity of the samples was measured in the temperature range between −50 and 350 °C with dc and ac methods at a measuring voltage of 0.1 V. The dc measurements were performed by conventional techniques. The impedance was measured with a HP 4192A analyzer (Agilent Technologies Inc., Palo Alto, CA, USA) between 10 Hz and 13 MHz. The spectra of impedance and electrical modulus were fitted simultaneously by a model using equivalent RC circuits with up to three elements.

3. Results

The mean grain size of the samples investigated is shown in Table 1. Whereas the specimens with 0.25 and 1.5 mol% La are coarse-grained with typical anomalous grain growth (AGG) of $BaTiO_3$, the sample with 3.0 and 5.0 mol% are fine-grained and only the latter shows grain growth up to 10 μm. Obviously, the specimens with higher La concentration were not sintered with optimum reducing conditions.

3.1. Coulometric investigation

A typical example for the coulometric measurement[a] of a sample with 1.5 mol% La is shown in Fig. 1. Dosing currents

---

[a] All coulometric data presented are corrected with respect to the influence of the furnace tube (alumina) and the sample pad (zirconia), since these oxides exhibit certain contributions to the totally measured oxygen exchange. For easier comparison, the curves are shifted to a common base line value of 8.0 mA.

Table 1
Mean grain size $\overline{d}$, onset temperature of peak (III), estimated oxygen uptake of peak (III) and calculated oxygen uptake which is consumed for the transformation of reduced to oxidized barium titanate of samples with a nominal composition of $0.98Ba_{1-x}La_xTiO_3 + 0.02TiO_2$

x	$\overline{d}$ (μm)	T_{onset} (°C) peak (III)	$\Delta x_O^{\text{uptake}}$ (exp.) peak (III)	$\Delta x_O^{\text{uptake}}$ (calc.) red. → ox. phase
0.0025	50			
0.015	60	1266	≈0.0030	0.0075
0.030	2	1244	≈0.016	0.0150
0.050[a]	8	1225	≈0.026	0.0250

The oxygen uptake is given as mole fraction.

[a] The samples with 5.0 mol% La were prepared without nominal excess of TiO_2, but contain an effective Ti excess of at least 1 mol% since they were fine-milled in water.

larger than the base line value of 8.0 mA mean oxygen uptake of the specimen and vice versa. During the heating cycle up to 1380 °C three different uptake peaks were detected which are marked by (I)–(III). A further peak (IV) starts immediately with the beginning of the cooling cycle, whereas the existence of peak (V) near 250 °C is not yet well established, since its amplitude does not exceed the fluctuations of the measuring signal significantly. This peak does not exist at 0.25 mol% La.

To compare the specimens with different donor concentration, the dependence of the dosing current on temperature is shown in Fig. 2 for the heating cycle. All specimens were cooled down immediately after reaching the maximum temperature except for the sample with 5.0 mol% La (45 min soaking time). The measurements were exactly reproduced several times and also with lower maximum temperatures (not shown in Fig. 2) to investigate the possible changes in microstructure and electrical properties dependence on the maximum reoxidation temperature.

Two tendencies of the development of the reoxidation peaks are observed. Whereas peak (I) decreases with increasing donor content and vanishes at 3.0 and 5.0 mol% La, peak (III) shows the opposite behaviour. At 0.25 mol% La it is not well developed or appears as a weak peak eventually hidden because of the overlap with an oxygen expelling effect. At higher La concentrations peak (III) is well developed and exhibits a distinct onset temperature that somewhat decreases with increasing La content (Table 1). The onset points were determined by the intersection of the corresponding linear curve sections. Table 1 also shows the amount of oxygen uptake corresponding to peak (III), which was roughly estimated by fitting with a Gauss curve.

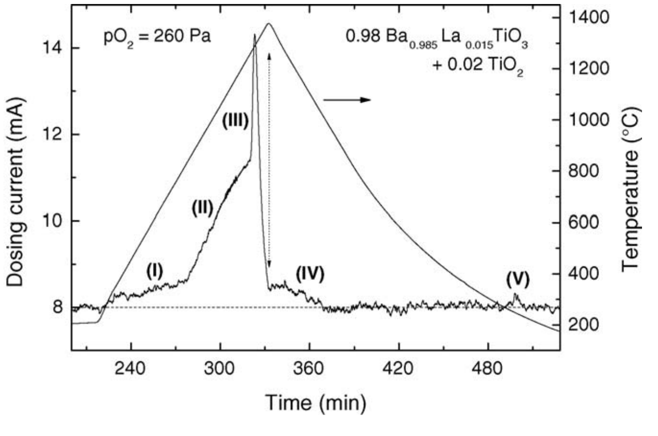

Fig. 1. Dosing current of the coulometric measuring cell and the temperature of a $BaTiO_3$ sample doped with 1.5 mol% La as a function of time during the complete reoxidation cycle. Marks (I)–(V) are explained in the text.

Peak (II) also increases with increasing La content and shows an onset temperature of about 800 °C for the specimens with 0.25 and 1.5 mol%. The samples with higher La concentration do not exhibit such clear onset behaviour of peak (II). It seems that it is shifted to somewhat higher temperatures.

3.2. TEM investigation

The reoxidation of the bulk of the donor-doped $BaTiO_3$ grains caused changes in their microstructure, which were detected by TEM. Fig. 3 shows a TEM micrograph of the area of a $BaTiO_3$ matrix grain with small precipitates corresponding to the specimen with 1.5 mol% La in Figs. 1 and 2. The precipitates were up to about 100 nm in size. EDS analysis of the precipitates prove

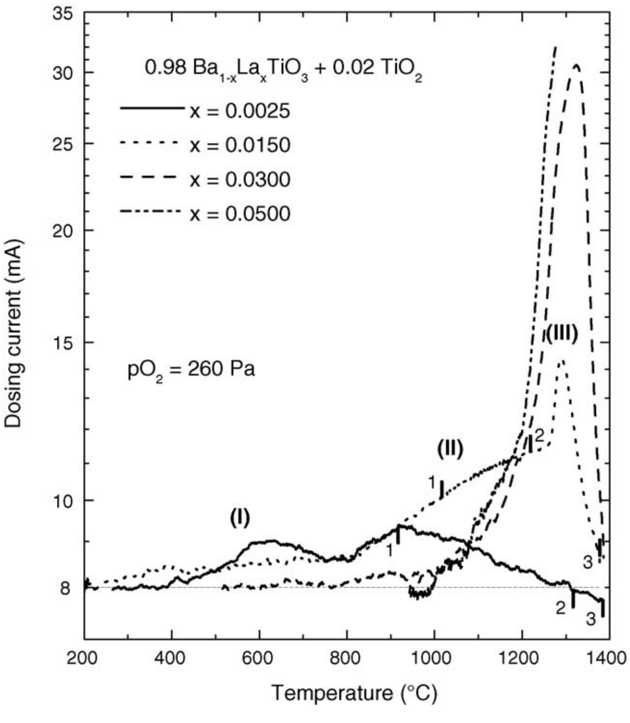

Fig. 2. Dosing current of the coulometric measuring cell as a function of temperature (heating cycle) for $BaTiO_3$ samples doped with 0.25–5.0 mol% La. Marks (I)–(III) are explained in the text. Marks 1–3 denote the maximum reoxidation temperature of samples, mentioned in the text.

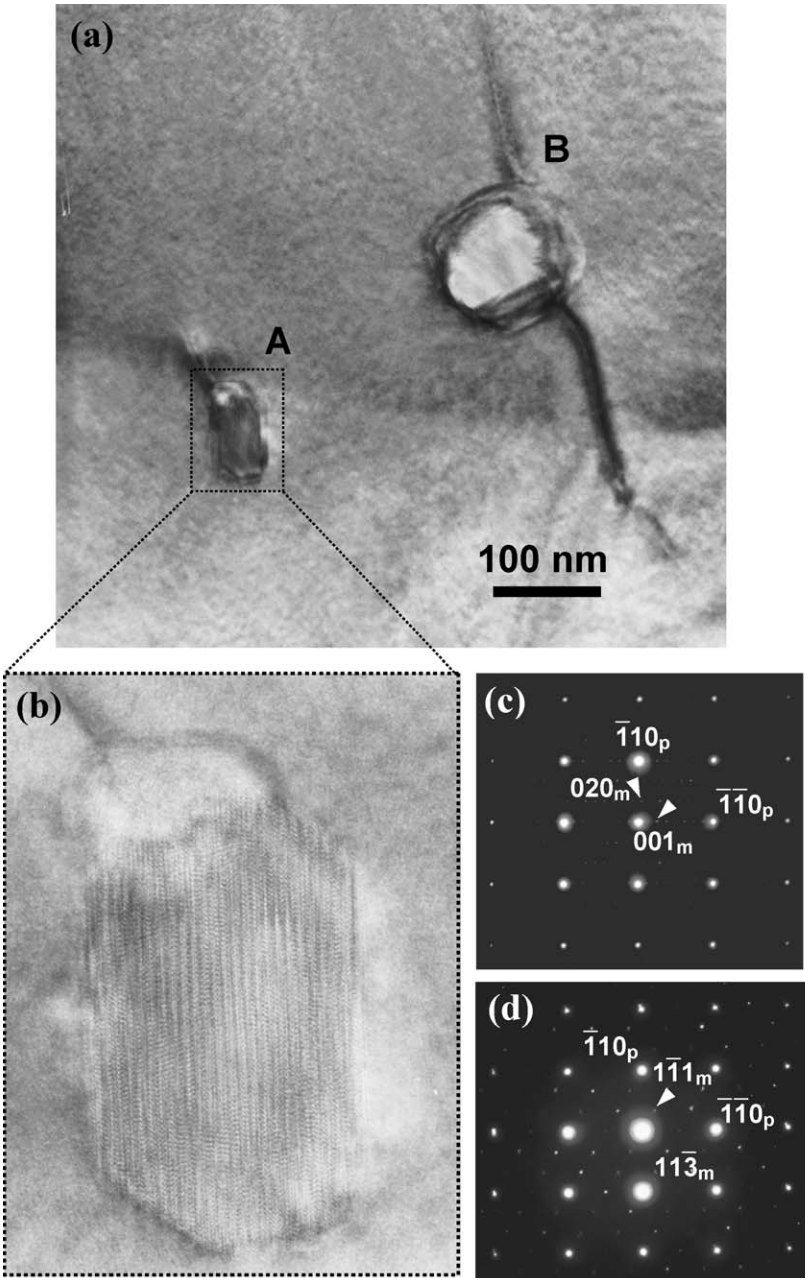

Fig. 3. Precipitates of the monoclinic compound $Ba_6Ti_{17}O_{40}$ (m) located inside the perovskite (p) grain of the 1.5 mol% La-doped $BaTiO_3$ sample, reoxidized by heating to 1377 °C in an atmosphere with 260 Pa of oxygen partial pressure. (a) Bright field image; (b) HREM image of the precipitate marked in (a) by A. (c) Electron diffraction pattern taken at the area of the grain marked in (a) by A. (d) Electron diffraction pattern taken at the area of the grain marked in (a) by B.

that they were Ti-rich compared to $BaTiO_3$, while their electron diffraction patterns (Fig. 3(c) and (d)) matched the structure of the monoclinic $Ba_6Ti_{17}O_{40}$ compound ($a = 0.989$ nm, $b = 1.712$ nm, $c = 1.893$ nm, $\beta = 98.71°$, space group $C2/c$).[16] They had a defined orientational relationship with the $BaTiO_3$ perovskite matrix, strongly suggesting that they were precipitated and not included into grains during grain growth. From the electron diffraction pattern shown in Fig. 3(c), which was taken from the region of the grain with the precipitate marked in Fig. 3(a) with A, the orientational relationship between the monoclinic compound $Ba_6Ti_{17}O_{40}$ (marked with m in Fig. 3(c)) and the perovskite matrix (marked with p in Fig. 3(c)) can be directly derived to be the same as already reported in Refs.[17,18]. The precipitates were present only in certain parts of the matrix grains, while other parts of the same grains were intact, free of any precipitates. No Ti-rich precipitates can be detected in the matrix grains of the samples, which were reoxidized during the coulometric measurement up to 1217 °C.

3.3. Electrical properties

3.3.1. dc electrical resistivity

Fig. 4 shows the dependence on the temperature of the dc electrical resistivity of samples, with 0.25, 1.5 and 5.0 mol% La,

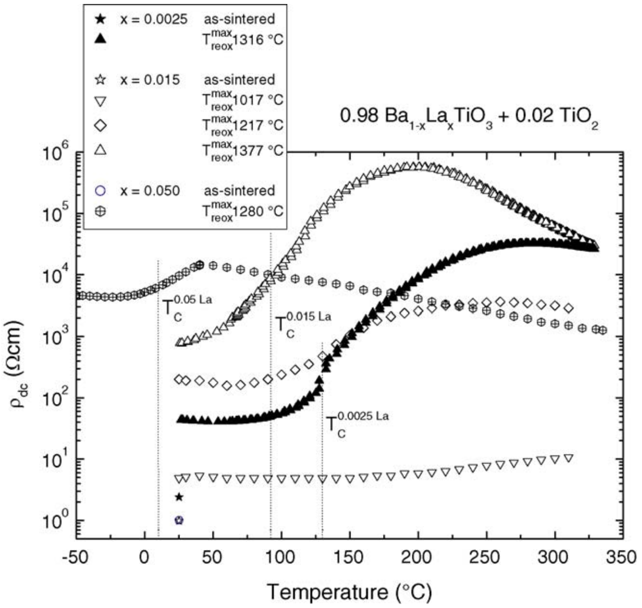

Fig. 4. Electrical resistivity ρ_{dc} dependence on temperature for $BaTiO_3$ samples doped with 0.25–5.0 mol% La. The ferroelectric phase transition temperatures are indicated by dotted lines.

after the reoxidation procedure up to different maximum temperatures together with the room temperature resistivity of the as-sintered samples before the reoxidation step. The curves with the highest reoxidation temperatures correspond to the samples for which coulometric data are shown in Figs. 1 and 2. Whereas the 1.5 mol% La-doped sample with a maximum reoxidation temperature of 1017 °C exhibits increased resistivity without PTCR effect, heating up to 1217 and 1377 °C causes PTCR behaviour of one and three orders of magnitude, respectively. The room temperature resistivity of the 3.0 mol% La-doped sample changes from 4.5 Ω cm to 20 kΩ cm after reoxidation and shows no PTCR behaviour near/above 64 °C, the sample's phase transition temperature, T_{tr}, ferroeletric–paraelectric.[20] The sample with 5.0 mol% La ($T_{tr} \approx 10$ °C) exhibits only a weak PTCR effect but its resistivity at T_{tr} is clearly lower compared to the 3.0 mol% doped sample.

3.3.2. Impedance spectroscopy

Impedance spectra were measured from room temperature until the temperature of the maximum resistivity $T(\rho_{max})$ of respective specimens. Fig. 5 shows an example for 1.5 mol% La-doped samples with maximum reoxidation temperatures of 1217 and 1377 °C, respectively. According to the structural model proposed,[10] an electrical model of equivalent parallel RC circuits with up to three elements was used. Since the time constants $\tau = RC$ of the different contributions can span over several orders, both complex quantities: impedance Z^* and electrical modulus $M^* = i\omega C_0 Z^*$ (ω, angular frequency; $C_0 = 1$ F) were fitted simultaneously. To get satisfying fitting results, a modified impedance formula

$$Z^* = \frac{R}{1 + (i\omega\tau)^{\beta}} \quad (1)$$

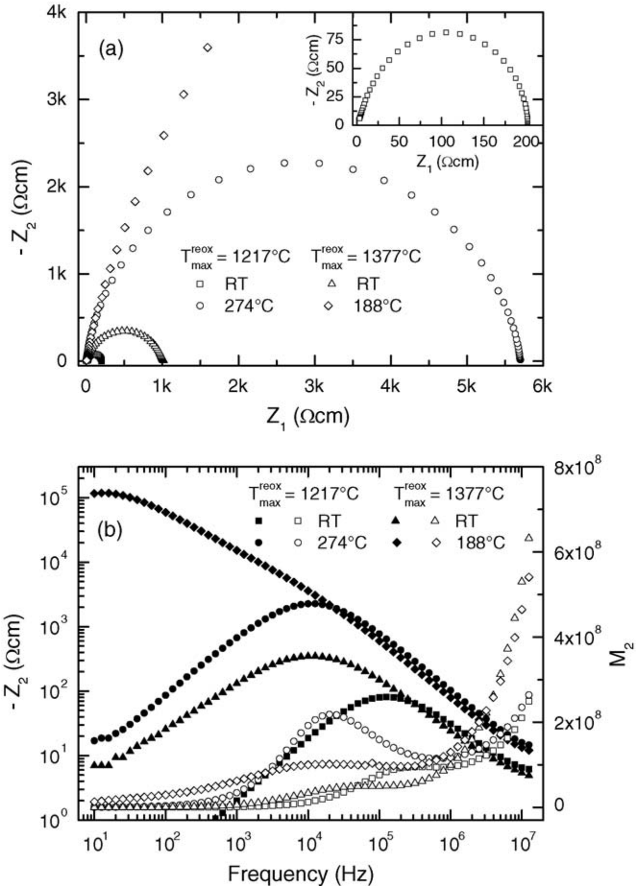

Fig. 5. Impedance data of 1.5 mol% La-doped $BaTiO_3$ samples for maximum reoxidation temperatures of 1217 and 1377 °C, measured at room temperature and at the temperature of maximum resistivity, respectively. (a) Complex impedance plane. (b) Spectra of the imaginary part of impedance Z_2 (full symbols) and electrical modulus M_2 (open symbols).

with the parameter $\beta \neq 1$ was used. This procedure is sometimes described in the literature as the use of a "constant phase element" instead of the capacity C.[21] $\beta = 1$ corresponds to a pure RC element. This parameter has no direct physical meaning and should not differ too much from 1. Table 2 shows selected fitting results, namely the resistivities of the RC elements, of the specimens which were introduced already above. Included are only the values for room temperature and for $T(\rho_{max})$, which is sufficient for the discussion of the PTCR properties of the different contributions.

4. Discussion

Three different mechanisms for oxygen uptake during the reoxidation process can be distinguished[10]:

(A) Filling up of the oxygen vacancies which are present in the reduced samples $(BaTi^{x/4+}_{1-x}Ti'^{/3+}_{x}O_{3-x/2}(V_O^{\bullet\bullet})_{x/2})$ according the reaction

$$V_O^{\bullet\bullet} + 2e' + \tfrac{1}{2}O_2 \downarrow\rightarrow O_O^x. \quad (2)$$

Following the defect models of donor-doped $BaTiO_3$,[4,19] the concentration of oxygen vacancies which are present

Table 2
Fitting results of impedance spectra of samples corresponding to those of Table 1

x	$T_{\mathrm{max}}^{\mathrm{reox}}$ (°C)	$\rho_{\mathrm{max}}/\rho_{\mathrm{RT}}$	$T_{\mathrm{measuring}}$ (°C)	ρ_{total} (Ω cm)	ρ_1 (Ω cm)	ρ_2 (Ω cm)	ρ_3 (Ω cm)
0.0025	935	3	RT	5.5	1.5	4.0	
			285	16	4.0	12	
	1316	570	RT	43	3.0	40	
			285	24.7k	6.3	24.7k	*
	1384	1020	RT	72	3.3	69	
			269	73.4k	10	73.4k	*
0.0150	1017	1	RT	4.0	1.0	2.5	
			265	3.2	1.0	2.2	
	1217	28	RT	203	2.8	200	
			274	5.70k	1.7	5.70k	*
	1377	370	RT	1008	13	184	811
			188	374k	5.0	4.00k	370k
0.0300	1386		RT	20.4k	3.0	375	20.0k
0.0500	1282[a]		RT	21.1k	4.1	516	20.6k

RT: room temperature. The asterisks are explained in the text.
[a] Holding time: 45 min.

in the reduced material decreases with increasing donor concentration as $\sim[\mathrm{La_{Ba}}]^{-n}$. n is between 0.5 and 1 in the range of the supposed freezing temperature of the V_O concentration between 600 and 1000 °C. Thus, $\Delta x_{\mathrm{O}}^{\mathrm{uptake\text{-}A}} \sim [\mathrm{La_{Ba}}]^{-n}$.

At temperatures above 1300 °C new V_O are formed by thermal energy and oxygen release occurs.[22] The reversibility of this last process is shown by the oxygen uptake peak (IV) appearing immediately at the beginning of the cooling cycle.

(B) Transformation of the reduced phase of $BaTiO_3$, where donors are electronically compensated ($\mathrm{Ba_{1-x}D_x{}^{\bullet}Ti^{4+}{}_{1-x}Ti^{3+}{}_xO_3}$) into oxidized phase with formation of metal vacancies ($\mathrm{Ba_{1-x}D_x{}^{\bullet}Ti^{x/4+}{}_{1-x/4}(V_{Ti}{}^{''''})_{x/4}O_3}$). The reduced phase is a non-equilibrium one at the oxygen partial pressure of 260 Pa in the surrounding atmosphere compared to the equilibrium oxidized phase (see Fig. 6). The process (B) could be described by the reaction:

$$\mathrm{Ba_{1-y}La_y{}^{\bullet}Ti^{x}_{1-y}Ti'_yO_3} + \frac{y}{4}\mathrm{O_2}\downarrow$$
$$\rightarrow \left(1-\frac{3y}{22}\right)\mathrm{Ba_{1-y}La_y{}^{\bullet}Ti^{x}_{1-(y/4)}(V_{Ti}{}^{''''})_{y/4}O_3}$$
$$+\frac{y}{44}\mathrm{Ba_6Ti_{17}O_{40}}. \tag{3}$$

This reaction needs oxygen which amount is proportional to the donor concentration $[\mathrm{La_{Ba}}]$ and $\Delta x_{\mathrm{O}}^{\mathrm{uptake\text{-}B}} = (1/2)\,[\mathrm{La_{Ba}}]$.

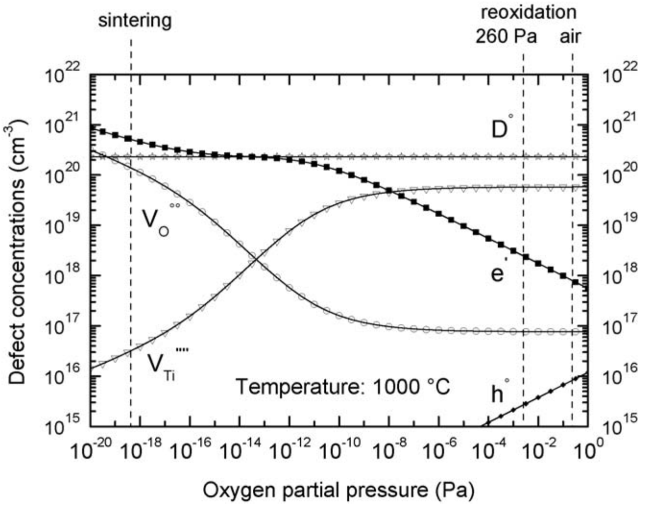

Fig. 6. General scheme of the equilibrium defect concentrations for donor-doped $BaTiO_3$ as a function of the oxygen partial pressure at 1000 °C.

(C) Due to the attractive force between oxygen and the surface of $BaTiO_3$, oxygen can be adsorbed at outer and inner (grain boundary) surfaces of the ceramic specimen. Since the attractive force is weak compared with the thermal energy at higher temperatures, adsorption takes place probably only during the cooling cycle whereas increasing temperatures cause the reverse desorption process. Both processes can only occur if the grain boundary diffusivity of oxygen is sufficiently large. This should be the case at rather low temperatures when bulk diffusion, which is the limiting oxygen transport process of mechanisms (A) and (B), is still negligible. Since adsorption is a surface process the amount of adsorbed oxygen is proportional to d^2 (d, mean grain size). If a monolayer of adsorbed oxygen atoms is assumed, the amount of oxygen which could be taken up by grain boundary adsorption can be estimated to $\Delta x_{\mathrm{O}}^{\mathrm{uptake\text{-}C}} = 3 \times 10^{-7}$ ($d \approx 50\,\mu$m). This amount should be detectable by oxygen coulometry if the process is not excessively smeared over a broad temperature range. Actually, the coulometry data presented give no evidence of a signal which could be related to a grain boundary adsorption process, if we disregard peak (V) in Fig. 1.

The electrical data of the 1.5 mol% La-doped sample (Fig. 4, Table 2) showed no changes in the electrical properties related to grain boundaries (PTCR effect), while TEM analysis showed that no changes occurred in the microstructure, which holds in both cases for samples which were reoxidized at a maximum temperature of 1017 °C. On the basis of those facts, it could be concluded that the filling up of the oxygen vacancies is related to the peak (I) in the coulometric curves (Figs. 1 and 2).

Because of the obvious proportionality between the amounts of oxygen uptake of peaks (II) and (III) and the donor concentration (Fig. 2, Table 1), these peaks are attributed to the oxidation of the reduced phase according Eq. (3). The opposite dependence of peak (I) on the donor concentration is also in accordance with the presumption that it is attributed to the annihilation of oxygen vacancies.

In order to change the donor compensation mechanism from electronic compensation (reduced phase) to the compensation with the ionized cationic vacancies (oxidized phase), some cations should be expelled from the solid solution. Due to the formation of Ti vacancies, the $Ba_6Ti_{17}O_{40}$ compound is precipitated.[17] Obviously, the reoxidation process is divided into two kinetically different processes, related to two peaks: (II) and (III) in the coulometric curves (Figs. 1 and 2).

(a) First, at lower temperatures, only the surroundings of the grain boundaries are reoxidized. In this case, the excess cations are precipitated at the grain boundaries. If Ti vacancies form in the vicinity of the grain boundaries, the $Ba_6Ti_{17}O_{40}$ compound will precipitate at the grain boundaries and triple points, where it cannot be differentiated from that compound already present there due to an excess TiO_2 in the starting composition. Because of the very low Ti diffusion coefficient,[23] this process takes place only in the direct vicinity of the grain boundaries and oxygen is provided by grain boundary diffusion. If Ba vacancies form in the vicinity of the grain boundaries, excess Ba precipitated at the grain boundaries will immediately react with the $Ba_6Ti_{17}O_{40}$ phase at the grain boundaries.

(b) At higher temperatures, oxidation of the grain interior is expected. In this case, the oxygen lattice diffusion inside the grain is combined with precipitation of the $Ba_6Ti_{17}O_{40}$ compound inside the grains.[10,17] This process is controlled by the oxygen transport inside the grain by bulk diffusion. The precipitation of the Ti-rich compound could occur everywhere inside the grain since the diffusion paths of Ti to the precipitate are rather short.

TEM analysis of the 1.5 mol% La-doped $BaTiO_3$ sample reoxidized during coulometric measurement up to maximal temperature of 1217 °C, just before the onset of the peak (III), showed no precipitates in the bulk. The precipitates were observed only after the reoxidation of the sample above the peak (III) in the coulometric curve (Fig. 3). In agreement with those facts, peak (II) was attributed to the reoxidation in the vicinity of the grain boundaries with the precipitation of extra cations to the grain surfaces, whereas the peak (III) was ascribed to the reoxidation of the grain interior near with the precipitation of the Ti-rich phase inside the grains. The oxygen transport by bulk diffusion causes the higher onset temperature of process (b). The rather abrupt onset of peak (III) could indicate that the precipitation reaction (3) is triggered by an activation energy. The systematic decrease of the onset temperature with increasing La concentration (Table 1) can be caused by the dependence of the chemical oxygen diffusion coefficient on the La content. The diffusivity has a minimum near 0.3 mol% and increases again with increasing donor concentration.[22] This phenomenon also could explain why the 0.25 mol% La-doped sample shows no or, at least, a rather weak peak (III), since there is not enough time to transport a measurable amount of oxygen to maintain process (b).

Due to the very large grains of the samples investigated by TEM, it is not possible to identify exactly, which parts of the grains were reoxidized. But according the discussion of process (b) the formation of reoxidized phase begins near the grain boundary and proceeds toward the centre of the grain. Hence, fine-grained ceramics like the 3.0 mol% La-doped sample are reoxidized much faster than the coarse-grained material.

The amount of oxygen uptake of process (b), roughly estimated by a Gauss-fit of peak (III), is shown in Table 1 together with the expected value for a complete transformation of the grain matrix into oxidized phase. While the sample with 1.5 mol% La shows the expected partial transformation into an oxidized phase, exhibiting a well developed PTCR behaviour, the samples with 3.0 and 5.0 seem to be completely transformed. Otherwise the samples are not insulating and the 5.0 mol% doped sample even exhibits a weak PTCR effect. This can be explained by the remaining oxygen vacancies since the samples being reoxidized at 260 Pa and not in air (20 kPa) and/or by an incorrect baseline of the Gauss-fit of peak (III).

The electrical data generally confirm the discussion above. The question remains as to which oxygen uptake processes determine (and in which manner) the development of the potential barrier, which is crucial for the PTCR behaviour and also for other grain boundary controlled electronic transport properties. For this investigation, the samples with 0.25 and 1.5 mol% La were reoxidized at different maximum temperatures. The resulting PTCR parameter ρ_{max}/ρ_{RT} is shown in Table 2 and the corresponding maximum temperatures are indicated on the coulometric measuring curves (see Fig. 2).

Obviously, reoxidizing without a completed process (a) (mark 1 in Fig. 2, middle of peak (II)) cannot produce a potential barrier and a following PTCR effect, whereas a reoxidation including process (b) is not necessary. The 1.5 mol% La-doped sample already exhibits a considerable PTCR effect without the formation of an oxidized phase in the bulk (mark 2 on curve with $x = 0.015$). The completely reoxidized sample has, quantitatively, only a slightly increased PTCR effect. For further discussion a schematic grain boundary model is introduced. Fig. 7 shows hypothetical concentration profiles of donors, titanium vacancies and electrons together with the total charge density which is significantly influenced by the negative space charge of O^{2-} adsorbed at the grain boundary. This negative space charge causes the potential barrier. Other sources of negative space charge like cation vacancies or segregated foreign acceptors are not considered. Excess barium vacancies proposed by Daniels et al.[3] as being formed by the reaction with Ti-rich sec-

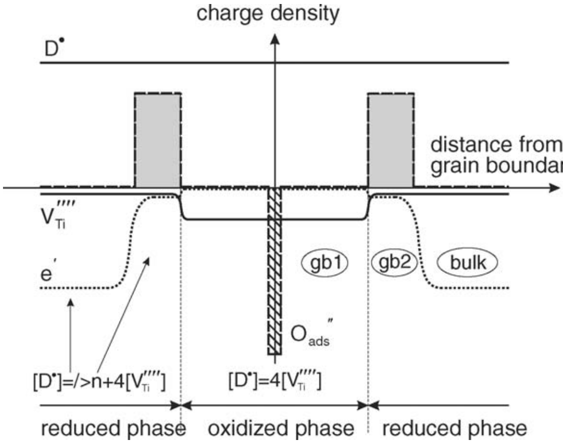

Fig. 7. Schematic grain boundary model for semiconducting $BaTiO_3$ ceramics: dependence of defect concentrations and total charge density on the distance to the grain boundary.

ondary phase at the grain boundary are discussed in the literature but now considered to be less likely (see, e.g. Ref.[24]). To explain an excess of titanium vacancies, i.e. $[V_{Ti}{''''}] > (1/4)[La_{Ba}{}^{\bullet}]$ is difficult, since the only driving force to create them is the transformation from the reduced to the oxidized $BaTiO_3$ phase. Of course, the long-standing question about the nature of the negative space charge is still not satisfactorily answered. To simplify the model, oxygen vacancies which increase the electron density and which are still present at an oxygen partial pressure of 260 Pa are also not considered.

The proposed model (Fig. 7) describes the status of a well-developed outer shell of oxidized phase which holds only for a later reoxidation stage (e.g. mark 3, $x = 0.015$ in Fig. 2).

Three electrically different regions can be distinguished.

1. Bulk region with relatively high electron density where the donor is compensated more by electrons than by titanium vacancies, depending on the conditions during reducing sintering (marked as bulk in Fig. 7).
2. The region of oxidized phase in the outer shell of the grain with dominating vacancy compensation and low electron density (marked as gb1 in Fig. 7).
3. The region between bulk and gb1, where the titanium vacancy concentration has the same value as that of the bulk, but the electron density is lowered, since the negative space charge at the grain boundary has to be compensated globally by the positive donors in that region (marked gb2 in Fig. 7). Region gb2 corresponds to the electron depletion layer introduced by Heywang[1] and its thickness is determined by the effective donor density of the bulk ($[D^{\bullet}] - [V_{Ti}{''''}]$) and the surface density of adsorbed oxygen.

Thus, the fitted resistivities (ρ_1, ρ_2, ρ_3, Table 2) can be interpreted in terms of the electrical properties of the grain regions discussed above. Obviously, resistivity ρ_1 as the distinctly lowest value can be assigned to the bulk region. It should be noted, that this value reflects the true material property, only if the bulk size is significantly larger than the thickness of the other two regions, which is only the case for the coarse-grained samples ($x = 0.0025$, 0.015). The values of ρ_2 and ρ_3, respectively, as properties of layers inside the grain have to be corrected to the ratio of the grain size to the layer thickness, which is unknown; for the discussion, the absolute values are not important.

The samples reoxidized at T_{max} of 935 and 1017 °C, respectively, practically do not exhibit PTCR behaviour. This means that significant oxygen adsorption, which causes the potential barrier, only occurs if process (a) is sufficiently advanced, i.e. if a certain *saturation* of oxygen near the grain boundary, according to the tendency for the formation of oxidized phase, is reached, or, in other words, if the local sinks for oxygen transport into the grain disappear. The latter is of course more speculative.

As already mentioned above, reoxidation process (b) is not necessary to develop the PTCR effect and potential barrier, respectively. This is reflected by the fact that only the 1.5 mol% doped sample reoxidized at $T_{max} = 1377$ °C and the samples with 3.0 and 5.0 mol% La, which all show a distinct oxygen uptake peak (III), had to be fitted with three RC circuit elements. For all other samples a three-element-fitting was formally possible but the corresponding τ values of elements 2 and 3 were so similar, i.e. their dispersion frequencies overlapped so strongly that the coincidence between the measuring spectra and the two-element-model fitted just as well as the three-element-fit. That means, that the outer shell region gb1 of these samples is not or only weak developed. This is confirmed by the tendency that the impedance spectra at $T(\rho_{max})$ of the 0.25 mol% doped samples with high maximum reoxidation temperature (1316, 1384 °C) and the 1.5 mol% doped sample ($T_{max} = 1217$ °C) showed a weak indication of a somewhat better three-element-fit (only small difference in the χ^2 value, marked by (*) in Table 2).

The higher values of ρ_3 compared with ρ_2 give rise to the assumption that they are properties of region gb1, since the electron density in the oxidized phase is much lower than in the depletion layer gb2 of the reduced phase. The fitted data show that both regions contribute to the PTCR effect. It should be mentioned again that the non-insulating character of the oxidized phase is probably caused by the remaining oxygen vacancies in the material.

5. Conclusion

La-doped $BaTiO_3$ samples that were sintered in highly reducing atmosphere can be reoxidized at an oxygen partial pressure of 260 Pa to restore successfully the GBBL. During the heating cycle up to 1380 °C three oxygen uptake processes with different onset temperatures were detected. The first one, $T_{onset} \approx 250$ °C, is attributed to the filling of oxygen vacancies, whereas the second, $T_{onset} \approx 800$ °C, and the third, $T_{onset} \approx 1250$ °C, are caused by the transformation of the reduced phase of $BaTiO_3$ into the oxidized phase. During the first stage ($T > 800$ °C), the transformation takes place only in the direct vicinity of the grain boundary. In the second stage characterized by a sudden onset ($\approx$1250 °C) and the occurrence of Ti-rich precipitations, additionally, the grain interior is gradually oxidized. This process is controlled by the bulk diffusion of oxygen. It seems that the development of the GBBL only requires a sufficiently advanced formation of the oxidized phase at the grain boundary (first stage) whereas during the second stage the barrier height only increases. The correlation between the oxidation processes and the final electrical properties can only be discussed properly if the cooling cycle is included, since the potential barrier will be completely developed only during cooling by adsorption of oxygen at the grain boundary. This will be the subject of future investigations. The simultaneous fitting of the spectra of impedance and electrical modulus, and their dependence on temperature, allowed the separation of up to three electrically different regions: (1) bulk region of reduced phase, (2) electron depletion layer in the outer part of the reduced phase and (3) oxidized phase in the outer grain shell. Both regions (2) and (3) contribute to the PTCR effect, but region (3) is manifest in the spectra only if the reoxidation temperature exceeds about 1300 °C, which corresponds to the two stages of formation of the oxidized phase.

Acknowledgement

The work was done in the framework of the European COST programme, action 525 "Advanced electroceramics: Grain boundary engineering", project D/6 for which support is gratefully acknowledged.

References

1. Heywang, W., Resistivity anomaly in doped barium titanate. *J. Am. Ceram. Soc.*, 1964, **47**, 484–490.
2. Huybrechts, B., Ishizaki, K. and Takata, M., The positive temperature coefficient of resistivity in barium titanate. *J. Mater. Sci.*, 1995, **30**, 2463–2474.
3. Daniels, J., Härdtl, K. H., Hennings, D. and Wernicke, R., Defect chemistry and electrical conductivity of doped barium titanate ceramics. *Philips Res. Rep.*, 1976, **31**, 487–559.
4. Chan, N.-H. and Smyth, D. M., Defect chemistry of donor-doped $BaTiO_3$. *J. Am. Ceram. Soc.*, 1984, **67**, 285–288.
5. Wu, T.-B. and Lin, J.-N., Transition of compensating defect mode in niobium-doped barium titanate. *J. Am. Ceram. Soc.*, 1994, **77**, 759–764.
6. Morrison, F. D., Sinclair, D. C. and West, A. R., An alternative explanation for the origin of the resistivity anomaly in La-doped $BaTiO_3$. *J. Am. Ceram. Soc.*, 2001, **84**, 474–776.
7. Drofenik, M., Origin of the grain growth anomaly in donor-doped barium titanate. *J. Am. Ceram. Soc.*, 1993, **76**, 123–128.
8. Murakami, T., Nakahara, M., Miyashita, T. and Ueda, S., Effect of rare-earth ions on electrical conductivity of $BaTiO_3$ ceramics. *J. Am. Ceram. Soc.*, 1973, **56**, 294–297.
9. Drofenik, M., Oxygen partial pressure and grain growth in donor-doped $BaTiO_3$. *J. Am. Ceram. Soc.*, 1987, **70**, 311–314.
10. Makovec, D., Ule, N. and Drofenik, M., Positive temperature coefficient of resistivity effect in highly donor-doped barium titanate. *J. Am. Ceram. Soc.*, 2001, **84**, 1273–1280.
11. Hanke, L. and Schmelz, H., *Ceramic Cold Conductor with a Low Cold Resistance*. German Patent DE 3019098, 26 November 1981 (Siemens).
12. Chan, H. M., Harmer, M. P. and Smyth, D. M., Compensating defects in highly donor-doped $BaTiO_3$. *J. Am. Ceram. Soc.*, 1986, **69**, 507–510.
13. Makovec, D., Samardzija, Z., Delalut, U. and Kolar, D., Defect structure and phase relations of highly lanthanum-doped barium titanate. *J. Am. Ceram. Soc.*, 1995, **78**, 2193–2197.
14. Morrison, F. D., Sinclair, D. C. and West, A. R., Characterization of lanthanum-doped barium titanate ceramics using impedance spectroscopy. *J. Am. Ceram. Soc.*, 2001, **84**, 531–538.
15. Langhammer, H. T., Song, Q. M., Felgner, K.-H. and Abicht, H.-P., Investigations on the defect chemistry and the sintering of barium titanate ceramics by oxygen coulometry. *Solid State Sci.*, 2002, **4**, 197–203.
16. Negas, T., Roth, R. S., Parker, H. S. and Minor, D., Subsolidus phase relations in the $BaTiO_3$–TiO_2 system. *J. Solid State Chem.*, 1981, **9**, 287–307.
17. Makovec, D. and Drofenik, M., Microstructural changes during the reduction/reoxidation process in donor-doped $BaTiO_3$ ceramics. *J. Am. Ceram. Soc.*, 2000, **83**, 2593–2599.
18. Kraševec, V., Drofenik, M. and Kolar, D., Topotaxy between $BaTiO_3$ and $Ba_6Ti_{17}O_{40}$. *J. Am. Ceram. Soc.*, 1987, **70**, C-193–C-195.
19. Daniels, J. and Härtdl, K. H., Electrical conductivity at high temperatures of donor-doped barium titanate ceramics. *Philips Res. Rep.*, 1976, **31**, 489–504.
20. Morrison, F. D., Sinclair, D. C. and West, A. R., Electrical and structural characteristics of lanthanum-doped barium titanate ceramics. *J. Appl. Phys.*, 1999, **86**, 6355–6366.
21. Macdonald, J. R., *Impedance Spectroscopy*. Wiley, New York, 1987, p. 27.
22. Langhammer, H. T., Drofenik, M., Felgner, K.-H. and Abicht, H.-P., Investigation of semiconducting barium titanate ceramics by oxygen coulometry. *J. Electroceram.*, 2004, **13**, 793–797.
23. Yoo, H.-I. and Lee, C.-E., Two-fold diffusion kinetics of oxygen re-equilibration in donor-doped $BaTiO_3$. *J. Am. Ceram. Soc.*, 2005, **88**, 617–623.
24. Alles, A. B. and Burdick, V. L., Grain boundary oxidation in PTCR barium titanate thermistors. *J. Am. Ceram. Soc.*, 1993, **76**, 401–408.